THE JOURNAL OF BIOLOGICAL CHEMISTRY
Vol. 278, No. 36, Issue of September 5, pp. 33928–33935, 2003
Printed in U.S.A.

Cholesterol Impairs the Adenine Nucleotide Translocator-mediated Mitochondrial Permeability Transition through Altered Membrane Fluidity*

Received for publication, October 25, 2002, and in revised form, May 19, 2003
Published, JBC Papers in Press, June 23, 2003, DOI 10.1074/jbc.M210943200

Anna Colell‡, Carmen García-Ruiz‡§, Josep M. Lluis, Olga Coll, Montse Mari, and José C. Fernández-Checa§¶

From the Liver Unit, Institut de Malalties Digestives, Hospital Clínic y Provincial, Instituto Investigaciones Biomédicas August Pi Suñer and the §Department of Experimental Pathology, Instituto Investigaciones Biomédicas Barcelona, Consejo Superior de Investigaciones Científicas, Barcelona 08036, Spain

Mitochondrial permeability transition (MPT) has been proposed to play a key role in cell death. Downstream MPT events include the release of apoptogenic factors that sets in motion the mitochondrial apoptosome leading to caspase activation. The current work examined the regulation of MPT by membrane fluidity modulated upon cholesterol enrichment. Mitochondria enriched in cholesterol displayed increased microviscosity resulting in impaired MPT induced by atractyloside, a c-conformation stabilizing ligand of the adenine nucleotide translocator (ANT). This effect was dependent on the dose of cholesterol loaded and reversed upon the fluidization of mitochondria by the fatty acid derivative A_2C. Mitoplasts derived from cholesterol-enriched mitochondria responded to atractyloside in a similar fashion as intact mitochondria, indicating that a significant amount of cholesterol is still found in the inner membrane. The effects of cholesterol on MPT induced by atractyloside were mirrored by the release of intermembrane proteins, cytochrome *c*, Smac/Diablo, and apoptosis inducing factor. However, cholesterol loading did not affect the uptake rate of adenine nucleotide hence dissociating the function of ANT as a MPT-mediated protein from its adenine nucleotide exchange function. Thus, these findings indicate that the ability of atractyloside to induce MPT via ANT requires an appropriate membrane fluidity range.

The mitochondrial permeability transition (MPT)[1] involves a sudden and initially reversible increase to solutes with molecular mass up to 1,500 Da. The rapid change in permeability associated with transition causes mitochondrial depolarization, uncoupling of oxidative phosphorylation, release of intramitochondrial solutes, large amplitude swelling, and outer membrane rupture (1). This phenomenon is mediated by opening of a large conductance channel, the permeability transition pore, located at the contact sites between mitochondrial membranes (2). Although the molecular identity of this multiprotein complex is only partially defined, some of its core components have been identified which include the adenine nucleotide translocator (ANT), found in the inner membrane and the voltage-dependent anion channel (VDAC), located in the outer membrane. Other proteins believed to be involved are the peripheral benzodiazepine receptor, hexokinase II (a cytosolic protein), creatine kinase (located in the intermembrane space), cyclophiline D (located in the mitochondrial matrix), as well as Bax/Bcl-2-like proteins (3–5).

The MPT has been shown to function as a key device in the control of cell survival regardless of the phenotype of cell death (2, 6–8). Agents that induce or prevent MPT modulate cell survival (9–11). As a result of mitochondrial membrane permeabilization death-promoting factors are released from the intermembrane space, thereby stimulating the execution phase of the cell death program. Such factors include cytochrome *c*, which triggers the assembly of the cytochrome *c*/Apaf-1/procaspase-9 activation complex, called the apoptosome (12, 13); certain inactive caspases precursors (14, 15); heat shock protein 10, which favors apoptosome activation (16); AIF (17) and endonuclease G (18), both of which mediate the cleavage of DNA during caspase-independent cell death; Smac/DIABLO (19, 20) and Omi/HtrA2 (21) that ensure inactivation of caspase inhibitors called inhibitors of apoptosis (IAPs), and recently, pre-processed caspase-9 (22).

Although one of the consequences derived from MPT is the rupture of the outer membrane, some studies have pointed out that outer membrane permeabilization may occur in the absence of disrupted inner membrane (23–26). Indeed there is growing evidence supporting the MPT-independent release of cytochrome *c* during apoptosis primarily because of the rupture or permeabilization of the mitochondrial outer membrane. Although it remains unclear exactly how mitochondrial outer membrane permeabilization occurs by MPT, large pore opening, or even hyperpolarization subsequent to the closure of

* This work was supported in part by Research Center for Liver and Pancreatic Diseases Grants P50 AA11999 and 1R21 AA014135-01 funded by the United States National Institute on Alcohol Abuse and Alcoholism, Plan Nacional de I+D Grants SAF 2001–2118 and SAF2002–3564, Fondo Investigaciones Sanitarias, FISS 00–907, and Grants G03/015 Red Temática de Investigación Cooperativa and C03/02 Red Nacional de Investigación en Hepatología y Gastroenterología from the Instituto de Salud Carlos III. The costs of publication of this article were defrayed in part by the payment of page charges. This article must therefore be hereby marked "*advertisement*" in accordance with 18 U.S.C. Section 1734 solely to indicate this fact.

‡ Contributed equally to the results of this work.

¶ To whom correspondence should be addressed: Liver Unit, Institut de Malalties Digestives, Hospital Clínic i Provincial. C/ Villarroel 170., 08036 Barcelona, Spain. Tel.: 34-93-227-5709; Fax: 34-93-451-5272; E-mail: checa229@yahoo.com.

[1] The abbreviations used are: MPT, mitochondrial permeability transition; A_2C, 2-(2-methoxyethoxy)ethyl-8-(cis-2-*n*-octylcyclopropyl)octane; ANT, adenine nucleotide translocator; AIF, apoptosis inducing factor; ATR, atractyloside; CSA, cyclosporin A; DPH, 1,6-diphenyl-1,3,5-hexatriene; MAO, monoamine oxidase; PBR, peripheral benzodiazepine receptor; TMA-DPH, trimethylammonium 1,6-diphenyl-1,3,5-hexatriene; VDAC, voltage-dependent anion channel; BSA, bovine serum albumin; CHAPS, 3-[(3-cholamidopropyl)dimethylammonio]-1-propanesulfonic acid; MOPS, 4-morpholinepropanesulfonic acid.

VDAC (27), it represents a key event allowing the release of intermembrane proteins, *e.g.* cytochrome *c*, that initiate the apoptosome activation leading to cell death.

Many different factors regulate MPT including Ca^{2+} and ADP levels (28), matrix pH and $\Delta\Psi m$ (29, 30), mitochondrial energetic status (31, 32), lipid peroxidation (33), oxidative stress because of reactive oxygen species, and/or mitochondrial GSH depletion (33–36). In pathological conditions, one or several of these MPT-regulating factors may contribute to altered susceptibility to MPT. For instance, liver mitochondria from ethanol-fed rats showed enhanced susceptibility to MPT induced by different stimuli (37, 38). The underlying mechanisms for these observations are not completely understood and may include damage to lipids or proteins, decrease of respiratory chain components, depletion of mitochondrial GSH, and changes in the composition of mitochondrial lipids.

Recent studies have reported that induction of MPT in rat liver mitochondria was accompanied by an increase in mitochondrial membrane fluidity because of conformational change of pore forming protein(s) during the assembly of the pore (39). Therefore, because a key factor determining the physical properties of membranes is the cholesterol to phospholipid molar ratio, this study was undertaken to examine the influence of mitochondrial membrane dynamics on ANT-mediated MPT and subsequent release of intermembrane proapoptotic factors.

MATERIALS AND METHODS

Reagents and Antibodies—A_2C, atractyloside (ATR), cyclosporin A, BSA, cholesterol, *O*-phthalaldehyde, phenylmethylsulfonyl fluoride, CHAPS, pepstatin A, leupeptin, aprotinin, and *N*-acetyl-leucyl-leucyl-norleucine were purchased from Sigma. Hexane, propanol, and acetonitrile (high performance liquid chromatography grade) were purchased from Merck (Darmstadt, Federal Republic of Germany). TMA-DPH, DPH, 9-(anthroyloxy)stearic acid, and anti-cytochrome oxidase subunit II were obtained from Molecular Probes (Eugene, OR). Anti-Smac/Diablo antibody was purchased from Calbiochem. Anti-cytochrome *c* antibody (clone 7H8.2C12) was from Pharmingen (San Diego, CA). Rabbit antiserum anti-AIF and anti-VDAC antibody, antibody number 25, were generous gifts from G. Kroemer (Centre National de la Recherche Scientifique, Villejuif, France) and Dr. Y. Tsujimoto (Osaka University Graduate School of Medicine, Osaka, Japan), respectively.

Mitochondria Preparation and Functional Integrity—Rat liver mitochondria were isolated from liver homogenates by differential centrifugation (40). Alternatively, highly purified mitochondria were prepared by rapid centrifugation through Percoll density gradient as described in detail previously (41). Enrichment and recovery of mitochondria were ascertained by the specific activity of succinic dehydrogenase. Mitochondrial purity was confirmed by estimating the contamination with other subcellular organelles such as sinusoidal and canalicular plasma membranes, microsomes and lysosomes assessed by the activity of Na^+,K^+-ATPase, Mg^{2+}-ATPase, glucose 6-phosphatase, and acid phosphatase, respectively. Integrity was determined by the acceptor control ratio as the ADP-stimulated oxygen consumption over its absence using a Clark oxygen electrode with glutamate/malate or succinate as substrates for respiratory sites for complexes I or II.

Measurement of MPT—Large amplitude swelling was measured spectrophotometrically by recording absorbance at 540 nm. Isolated rat liver mitochondria (1 mg/ml) were suspended in a buffer consisting of 200 mM sucrose, 10 mM Tris-MOPS, 5 mM succinate, 1 mM potassium phosphate, 2 μM rotenone, 1 μg/ml oligomycin, 10 μM EGTA, pH 7.4, at 25 °C as described before (42). Opening of the pore was induced by the ANT ligand, ATR (100 μM), and prevented by preincubation with cyclosporin A (CSA) (5 μM).

Preparation of Mitoplasts—Mitoplasts were prepared as previously described (43). Briefly, to a suspension of 20 mg of mitochondrial protein/ml in 220 mM mannitol, 70 mM sucrose, 2 mM HEPES, and 0.05% BSA, pH 7.4, an equal volume of digitonin (2.4 mg/ml) in the same buffer without BSA was added. After incubation for 15 min at 4 °C, the sample was diluted three times, homogenized gently, and centrifuged for 10 min at 9,500 × *g*, and the pellet was resuspended in 3 volumes of buffer and centrifuged as before. The resulting supernatants were combined and centrifuged for 1 h at 144,000 × *g* to obtain the outer mitochondrial membrane. The efficiency of the procedure was verified by monitoring the MAO activity in the low speed pellet (mitoplasts) compared with the high speed pellet (outer membrane) or intact mitochondria from the oxidation of benzylamine (3.3 mM final concentration).

Mitochondrial Loading with Increasing Amounts of Cholesterol—Cholesterol-BSA complex was made by dissolving 50 mg of cholesterol in 5 ml of absolute ethanol as described (44). To the white solution obtained after addition of 5 ml of double distilled water, 2 g of BSA was added adjusting the pH to 7.3 and then centrifuged at 12,000 × *g* at 4 °C for 10 min. Ten to fifty μl of the cholesterol/BSA mixture was incubated at 4 °C with 50 mg of mitochondria protein for 1 min. Mitochondria were diluted 20 times with cold solution of 0.25 M sucrose, 1 mM EDTA, pH 7.3, and immediately recovered by centrifugation and washed three times, to eliminate excess cholesterol. Parallel control experiments were performed using only BSA. This procedure resulted in cholesterol loading from about 25 to 350% over basal levels.

Cholesterol Determination—The amount of cholesterol incorporated in mitochondria or mitoplasts was measured by high performance liquid chromatography (45). 10 mg of protein was saponified with alcoholic KOH in a 60 °C heating block for 30 min. No cholesterol was detectable in the remnant protein. After the mixture had cooled, 10 ml of hexane and 3 ml of distilled water were added and shaken to ensure complete mixing. Appropriate aliquots of the hexane layer were evaporated under nitrogen and used for cholesterol measurement. High performance liquid chromatography analyses were made using a Waters μBondapak C18 10-μm reversed-phase column (30 cm × 4 mm inner diameter), the mobile phase was 2-propanol/acetonitrile (50:50, v/v) at a flow rate of 1 ml/min.

Fluidization of Mitochondria—Mitochondrial suspension (2 mg/ml) was incubated in 10 mM Tris-HCl, pH 7.4, 150 mM KCl, 1 mM EDTA, with A_2C (125 nmol/mg of protein) from a stock solution of 12 mg/ml as described in detail previously (43). The suspension was incubated at 37 °C for 30 min and then washed twice by spinning at 9,500 × *g* for 10 min.

Measurement of Fluorescence Anisotropy—Fluidity of mitochondrial membranes was evaluated by fluorescence anisotropy of mitochondria-bound dyes, TMA-DPH, DPH, or 9-(anthroyloxy)stearic acid, as described in detail previously (43). Briefly, TMA-DPH or 9-(anthroyloxy)stearic acid (final concentration 3 μM) were injected into stirred mitochondrial suspensions (0.5 mg/ml) and the mixture was incubated for 30 min at 37 °C, whereas DPH (20 mM in tetrahydrofuran) was diluted 100 times with 10 mM Tris-HCl, pH 7.4, 150 mM KCl, 1 mM EDTA. Fluorescence polarization was measured in a Hitachi spectrofluorometer at wavelengths of 366 nm for excitation and 425 nm for emission for TMA-DPH or DPH, and 366 nm excitation and 440 nm emission wavelengths for 9-(anthroyloxy)stearic acid (43). The results are expressed as anisotropy units (r), where $r = (I_0/I_{90})/(I_0 + 2I_{90})$. I_0 and I_{90} represent the intensities of light when polarizers were in parallel or perpendicular orientation, respectively. Correction for light scattering and intrinsic fluorescence were routinely made by subtracting the signal obtained from identical but unlabeled samples and the fluorescence of the buffer plus label alone.

Western Blot Analysis of Cytochrome c, Smac/Diablo, and AIF—Mitochondrial supernatants and pellets were collected by centrifugation at 10,000 × *g* for 5 min at 4 °C. 20–25 μg of proteins were separated by SDS-PAGE (15% gel) and transferred to nitrocellulose filters. Blots were probed with anti-cytochrome *c* (mouse monoclonal antibody; clone 7H8.2C12, dilution 1:2000), anti-AIF (rabbit antiserum, dilution 1:2000), and anti-Smac/Diablo (rabbit polyclonal antibody, dilution 1:1 000). After a 1-h incubation with the primary antibody, bound antibodies were visualized using horseradish peroxidase-coupled secondary antibodies and ECL developing kit (Amersham Biosciences). Parallel aliquots were analyzed by immunoblotting for the release of cytochrome oxidase using monoclonal antibody anticytochrome oxidase subunit II to confirm the specificity of mitochondrial proteins release.

Adenine Nucleotide Transport Assay—The adenine nucleotide transport was measured in mitochondria by the atractyloside stop method. The initial rate of [^{14}C]ADP (55 mCi/mmol, Amersham Biosciences) transport (2.5–40 μM) into mitochondria was performed in exchange for endogenous mitochondrial ATP. The assay was initiated by the addition of mitochondrial suspension (30 mg/ml) in a final volume of 766 μl and terminated by addition of 60 nmol of atractyloside followed by addition of excess cold transport buffer (120 mM KCl, 20 mM Tris-HCl, pH 7.4, 1.1 mM $MgCl_2$, and 25 mM sucrose) and subjected to vacuum filtration (Millipore, 0.45 μm) to separate medium from mitochondria. Retained mitochondria in filters were washed twice with 2.5 ml of ice-cold buffer. The filters were dried and placed in 10 ml of Aquasol for scintillation counting.

Electron Microscopy—Two milligrams of mitochondria or mitoplasts were fixed in 3% glutaraldehyde, 10 mM sodium phosphate buffer, pH

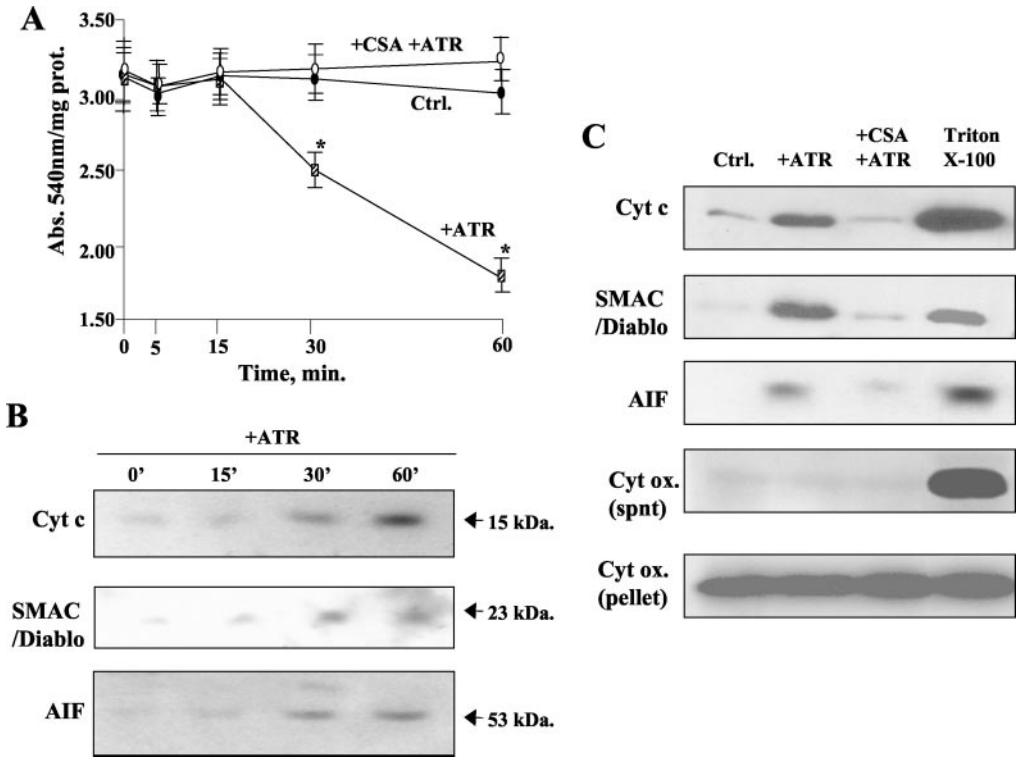

FIG. 1. **Mitochondrial swelling induced by atractyloside is accompanied by a release of apoptogenic factors.** *A*, isolated rat liver mitochondria (1 mg/ml) were incubated with 100 μM atractyloside (*ATR*) in the absence or presence of 5 mM CSA and changes in absorbance at 540 nm were examined as described under "Materials and Methods." Results are the mean of $n = 5$ individual experiments. *, $p < 0.05$ *versus* control. *B*, for the indicated periods of time supernatants were separated from the mitochondrial pellets by centrifugation and subjected to SDS-PAGE, followed by immunoblotting with anti-cytochrome *c* (*Cyt c*), anti-Smac/DIABLO, and anti-AIF antibodies as described under "Materials and Methods." *C*, CSA prevents atractyloside-induced release of cytochrome *c*, Smac/DIABLO, and AIF. The specificity of the release of these proteins was verified by levels of cytochrome oxidase (*cytochromeox.*) in supernatants using anti-cytochrome oxidase antibody. Parallel aliquots of mitochondria were treated with Triton X-100 (0.1%) examining the release of cytochrome *c*, Smac/DIABLO, and AIF. Representative immunoblots are shown of five individual experiments with similar results. *Ctrl*, control.

7.2, postfixed in 1% osmium tetroxide, dehydrated in graded steps of ethanol through propylene oxide, and embedded in SPURR. Finally, ultrathin sections were stained with uranyl acetate and lead citrate and photographed in a JEOL JEM 1010 electron microscope.

Statistical Analyses—Statistical analyses for comparison of mean values for multiple comparisons between mitochondrial preparations were made by one-way analysis of variance followed by Fisher's test.

RESULTS AND DISCUSSION

Cholesterol Enrichment Decreases Mitochondrial Membrane Fluidity and Impairs MPT Induced by ATR—Because recent studies have shown that MPT triggered by Ca^{2+}, histidine, or thiol reagents was accompanied by increased mitochondrial membrane fluidity (39), we examined the influence of membrane fluidity on MPT. To this end rat liver mitochondria were enriched in cholesterol as the cholesterol/phospholipid molar ratio has been shown to regulate membrane fluidity (46–50). ATR, a c-conformation stabilizing ANT ligand, has been shown to induce MPT (4, 51). Control mitochondria exposed to ATR underwent a time-dependent decrease in absorbance (Fig. 1*A*) and release of intermembrane proteins cytochrome *c*, Smac/DIABLO, and AIF (Fig. 1*B*). The addition of CSA, a MPT inhibitor (52), largely prevented the ATR-induced swelling, as well as the release of cytochrome *c*, Smac/DIABLO, and AIF (Fig. 1, *A* and *C*). To confirm the specificity of these effects, the levels of cytochrome oxidase subunit II were analyzed in the supernatants. As shown, cytochrome oxidase was undetectable in the medium unless mitochondria were permeabilized with Triton X-100 (Fig. 1*C*). These findings are in agreement with previous results (4, 51) thus validating the mitochondrial swelling induced by ATR as a characteristic feature of MPT.

We next examined the effect of cholesterol enrichment on the ability of ATR to cause mitochondrial swelling in relation to membrane fluidity. Cholesterol was incorporated into mitochondria by incubation with a BSA/cholesterol mixture as previously characterized (44). This approach increased cholesterol content over control levels (Figs. 2*A* and 3). Furthermore, the recovery of total mitochondrial protein matched the initial protein concentration of the mitochondrial suspension before the addition of the cholesterol-BSA complex, indicating that BSA was not bound to mitochondria and that it functions just as a carrier. Control experiments with BSA alone confirmed that BSA did not interfere with the different parameters analyzed (data not shown). To examine the dynamic properties of mitochondrial membranes after cholesterol enrichment, we analyzed the changes in the steady-state fluorescence anisotropy of mitochondria-bound TMA-DPH and DPH. The measurement of fluorescence polarization has been used as a common approach to determine the rotational diffusion freedom of the reported probes with respect to both the rate and the range or extent of the rotational motion (39, 46). The extent of depolarization of the exciting polarized light is a measure of the degree to which a population of photoselected probes lose their original orientation during the lifetime of the excited state (53). Mitochondria with increased cholesterol levels showed higher fluorescence polarization of TMA-DPH, a fluorescence dye incorporated in the membrane surface, compared with control mitochondria (Fig. 2*B*). Similar results were obtained using DPH, a fluorescence probe that is incorporated underneath the polar region of the bilayer (Fig. 2*B*). Interestingly, when mitochondria were incubated with the isomer of stearic acid labeled with the 9-anthroyloxy group to monitor fluidity in the core of

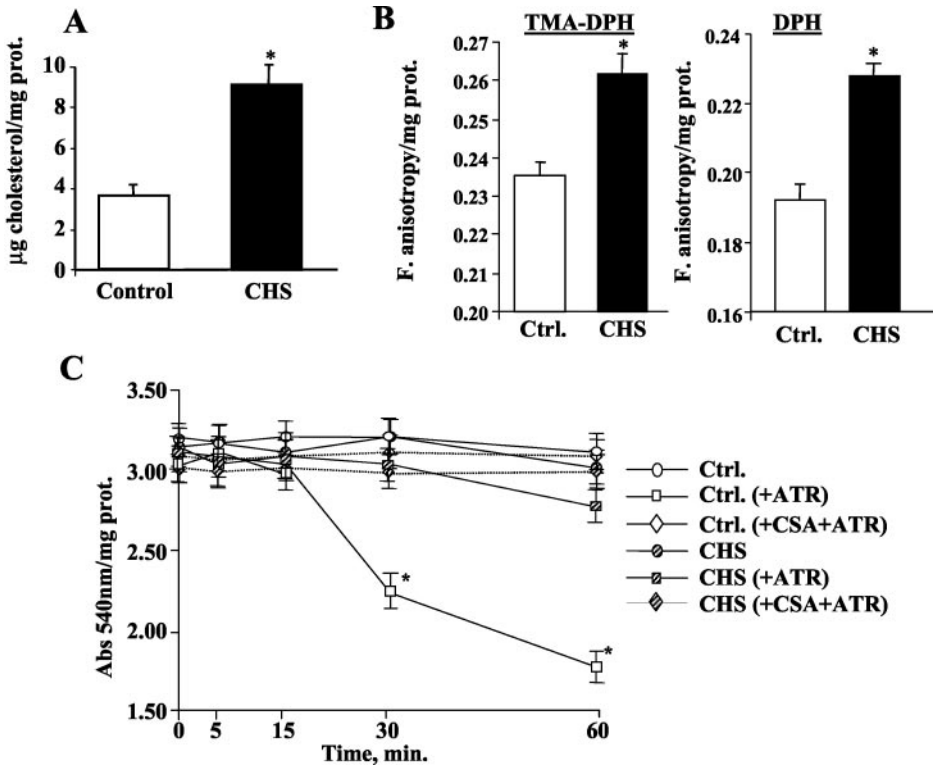

FIG. 2. **Effect of cholesterol enrichment on mitochondrial membrane fluidity and permeability transition.** *A*, mitochondria (50 mg of protein) were incubated for 1 min at 4 °C with a cholesterol-BSA complex (0.6 mmol of cholesterol), denoted as *CHS*. After the incubation, mitochondria were washed three times and cholesterol incorporation was measured as described under "Materials and Methods." *B*, control (*Ctrl*) and cholesterol-enriched mitochondria (*CHS*) (0.5 mg/ml) were labeled with TMA-DPH or DPH and fluorescence anisotropy was monitored at 366 nm (emission = 440 nm) using polarizing filters in both excitation and emission planes and normalized as per mg of mitochondrial protein. *C*, parallel aliquots were examined for changes in membrane permeability transition. ATR (100 μM) was added with or without a 5-min preincubation with CSA (5 μM) and mitochondrial swelling was measured by monitoring the optical density at 540 nm spectrophotometrically. Results are the mean ± S.D. of six different experiments. *, $p < 0.05$ *versus* control.

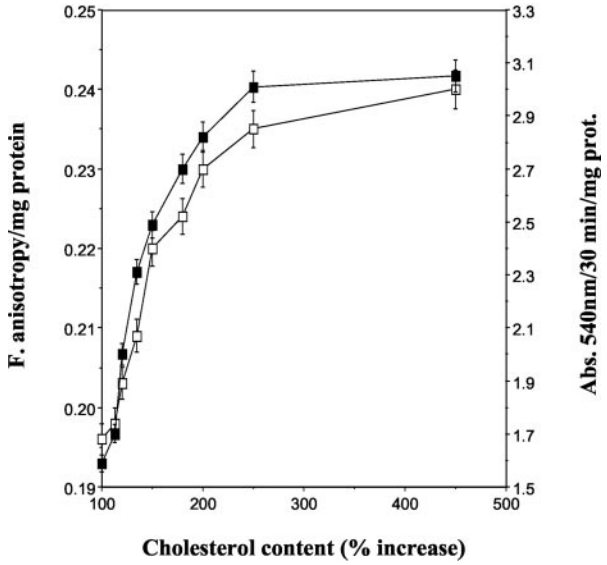

FIG. 3. **Relationship between cholesterol, membrane fluidity, and atractyloside-induced MPT.** Mitochondria were loaded with increasing amounts of cholesterol as indicated under "Materials and Methods." Mitochondrial aliquots were split and used for DPH fluorescence anisotropy measurements (*open squares*) and absorbance at 540 nm 30 min after atractyloside exposure (*closed squares*). Mitochondria were then processed for cholesterol determination and protein content and the cholesterol content expressed as percentage over control (cholesterol level 4.6 ± 1.2 μg/mg of protein). Results are mean ± S.D. of five to six independent experiments.

the lipid bilayer, no changes were observed in the steady-state fluorescence anisotropy from cholesterol-enriched mitochondria compared with control (data not shown). Cholesterol-enriched mitochondria incubated with ATR did not exhibit any significant change in optical density over time (Fig. 2*C*).

We next loaded mitochondria with increasing amounts of cholesterol to determine the dependence between cholesterol content, membrane fluidity, and MPT induced by atractyloside. As shown (Fig. 3), fluorescence anisotropy of mitochondria labeled with DPH increased as a function of the amount of cholesterol loaded, whereas the ability of ATR to induce MPT was impaired as reflected in absorbance changes over time after atractyloside exposure. The impairment of mitochondrial swelling in cholesterol-enriched mitochondria was accompanied with a decreased release of the apoptogenic factors, cytochrome *c*, Smac/DIABLO, and AIF induced by ATR (Fig. 4).

Because the cholesterol levels between the inner and outer mitochondrial membranes differ, and because ANT is located within the inner membrane (51), we next examined the relative distribution of cholesterol within mitochondrial membranes. Mitoplasts were prepared by selective solubilization of the outer membrane and used to determine the cholesterol levels and the ability of ATR to induce MPT. The removal of the outer membrane was assessed by monitoring MAO activity, an enzyme that localizes specifically in the outer membrane, and by electron microscopy. The MAO activity in low speed pellets containing mitoplasts was 10–15% of that found in intact mitochondria, with an outer/inner membrane ratio around 8.5 for both control and cholesterol-enriched organelles (Fig. 5*A*). Furthermore, electron microscopy confirmed the almost absence of outer membrane in both control and cholesterol-enriched mitoplasts compared with intact mitochondria (Fig. 5*B*). As shown, cholesterol levels in mitoplasts were lower than in corresponding intact mitochondria (Fig. 5*C*). However, the cholesterol content of mitoplasts from cholesterol-enriched mitochondria was higher than in mitoplasts from control mitochondria (Fig. 5*C*). Interestingly, cholesterol-enriched mitoplasts behaved in a similar fashion as intact mitochondria showing the resistance to ATR-induced swelling (Fig. 5*D*). Thus, although the main bulk of cholesterol is found in the outer membrane, the cholesterol incorporated in the inner membrane is enough to blunt ATR-induced MPT.

Measurement of fluorescence anisotropy of membranes labeled with fluorescent probes, *e.g.* DPH, has been widely used to monitor membrane fluidity changes that corresponds to the transition of membranes from gel to liquid crystalline state induced by cholesterol (46–50). In these prior studies, the

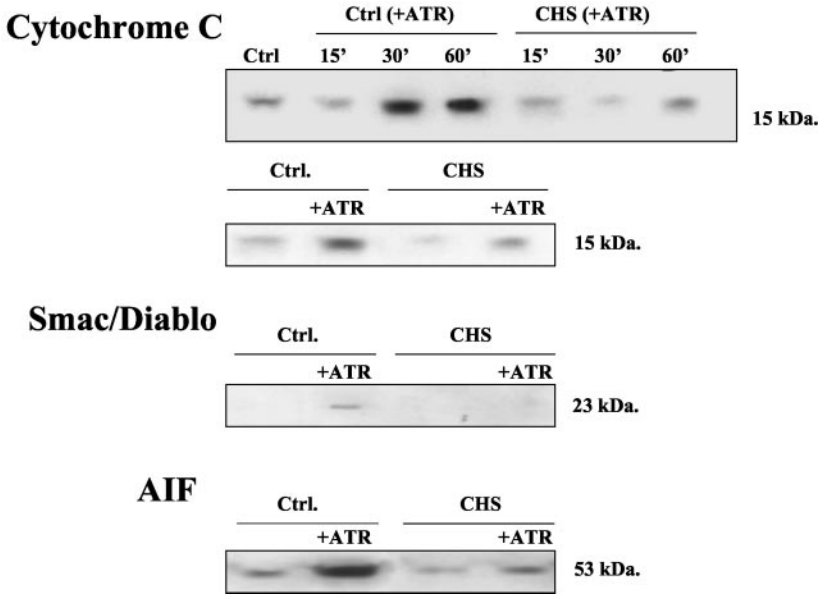

FIG. 4. **Cholesterol decreases the release of apoptogenic proteins induced by atractyloside.** Control (*Ctrl*) and cholesterol-enriched mitochondria (*CHS*) exposed for 1 h to ATR (100 μM) were pelleted and 25 mg of supernatant proteins were subjected to SDS-PAGE, followed by immunoblotting with anti-cytochrome *c* (*Cyt c*), anti-Smac/DIABLO, and anti-AIF antibodies as described under "Materials and Methods." Representative immunoblots are shown out of five individual experiments with similar results.

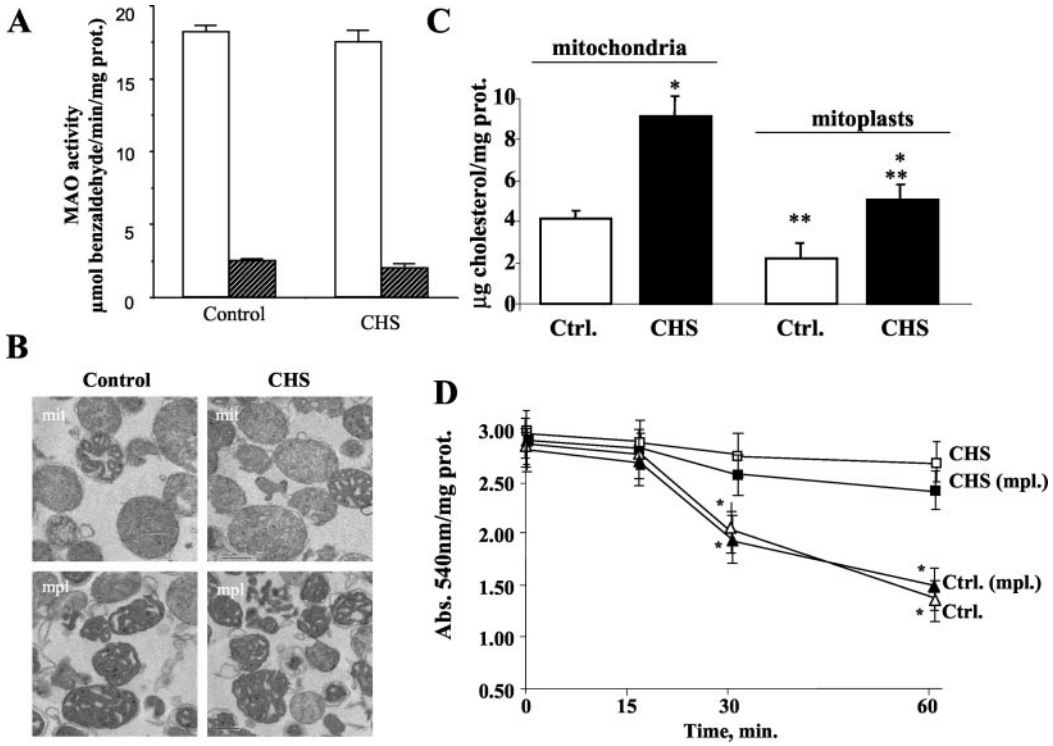

FIG. 5. **Membrane permeability transition induced by atractyloside on mitoplasts from cholesterol-enriched mitochondria.** Mitoplasts from control (*Ctrl*) and cholesterol-enriched mitochondria (*CHS*) were prepared by digitonin (120 μg/mg of mitochondrial protein) to remove outer membrane. *A*, solubilization of outer membrane was confirmed by determination of monoamine oxidase (*MAO*) in mitoplasts (*filled bars*) compared with intact mitochondria (*open bars*). *B*, intact mitochondria and mitoplasts were fixed as described under "Materials and Methods" for electron microscopy examination (×17,500). Isolated mitochondria showed an orthodox configuration (*mit.*) with both membranes compared with mitoplasts (*mpl*). *C*, cholesterol levels from mitochondria and mitoplasts. Levels of cholesterol in mitoplasts were corrected for the presence of intact mitochondria as estimated from the percentage of MAO activity found in mitoplasts. Results are the mean ± S.D. of six different experiments. *, $p < 0.05$ *versus* corresponding controls; **, $p < 0.05$ *versus* control mitochondria. *D*, membrane permeability transition was examined in control and cholesterol-enriched mitochondria and mitoplasts exposed to atractyloside (100 μM) as the decrease in absorbance at 540 nm. Results are the mean ± S.D. of six different experiments. *, $p < 0.05$ *versus* cholesterol-enriched organelles.

range of change in fluorescence anisotropy using DPH was similar to our present findings. For instance mitochondria from ischemic pig hearts exhibited higher mitochondrial cholesterol content (2-fold) and increased DPH fluorescence polarization (16% increase) (47). Moreover, membranes from HEK-OTR and HEK-CCKR cells loaded with cholesterol showed increased (13–16%) fluorescence anisotropy values for DPH (49). Fluorescence polarization of large multilamellar liposomes labeled with DPH increased gradually with increasing amounts of cholesterol (46). Thus taken together these findings indicate that cholesterol loading decreases mitochondrial membrane fluidity and that the function of ANT in MPT requires an appropriate membrane fluidity range.

Moreover, in addition to the mobility of fluorescence probes within membranes the lifetime of the excited state of the probe is another critical factor that can influence membrane fluidity

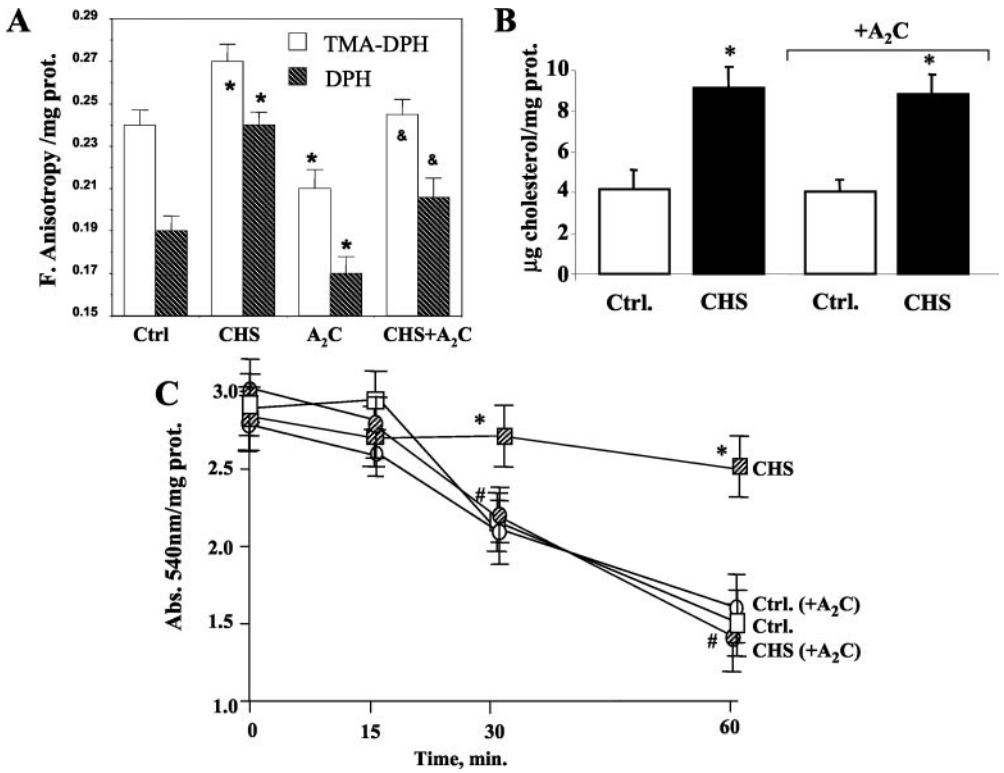

FIG. 6. **Fluidization of cholesterol-enriched mitochondria by A_2C.** Control (*Ctrl*) or cholesterol-enriched mitochondria (*CHS*) were exposed to the fluidizing fatty acyl derivative A_2C (125 nmol/mg of protein) for 30 min at 37 °C. *A*, samples were incubated with TMA-DPH and DPH and fluidity of mitochondrial membranes was evaluated by fluorescence anisotropy of mitochondria-bound dyes. Results are presented as mean ± S.D. ($n = 3$). *, $p < 0.05$ *versus* control. &, $p < 0.05$ *versus* cholesterol-enriched mitochondria. *B*, cholesterol content was analyzed by the *O*-phthalaldehyde method in control and cholesterol-enriched mitochondria with or without A_2C treatment. Results are presented as mean ± S.D. ($n = 3$). *, $p < 0.05$ *versus* control. *C*, membrane permeability transition induced by ATR (100 µM) was examined in control and cholesterol-enriched mitochondria fluidized by A_2C, analyzing changes in absorbance at 540 nm. Results are presented as mean ± S.D. ($n = 3$). *, $p < 0.05$ *versus* control. #, $p < 0.05$ *versus* CHS-enriched mitochondria.

measurements (46, 53). Previous studies using multilamellar liposomes loaded with increasing amounts of cholesterol reported no significant changes in the lifetime of the excited state of DPH (46). Thus, the differences in the steady-state fluorescence anisotropy of cholesterol-enriched mitochondria represent changes in the degree of static orientation constraint of the probe rather than changes in factors that modulate membrane fluidity such as the lifetime of the probe or the diffusion rates of the label.

Cholesterol Impairment of ATR-induced MPT Is Because of Increased Membrane Microviscosity—Having established that cholesterol hampers the ATR-induced MPT, we next examined whether this effect on ANT is mediated by cholesterol *per se* or through changes in the dynamic properties of mitochondrial membranes. To this end, we used A_2C, a fatty acid derivative that intercalates into the lipid bilayer resulting in its fluidization (54). The incubation of cholesterol-enriched mitochondria with this agent fluidized mitochondrial membrane to control values (Fig. 6*A*). Expectedly this strategy did not affect the cholesterol levels (Fig. 6*B*). Interestingly, the fluidization of cholesterol-enriched mitochondria by A_2C treatment restored the sensitivity of ANT to ATR as shown by the time-dependent optical density loss (Fig. 6*C*). To examine whether fluidization *per se* modulates the response to ATR, we analyzed the effect of A_2C on control mitochondria. The treatment of control mitochondria with A_2C resulted in further fluidization of mitochondria (Fig. 7*A*), but it did not affect ATR-induced mitochondrial swelling (Fig. 7*B*). These data establish that the modulation of cholesterol on ATR-induced mitochondrial swelling through ANT is exerted through alteration of membrane fluidity and that a critical fluid environment is necessary for optimal MPT induction by ATR.

ATR acts on ANT from the cytosolic face of the protein inducing the so called c-conformation. Because the affinity of ATR for ANT is in the nanomolar range (51), we would expect a saturation of the binding sites of ANT at the concentration of ATR used in our conditions (100 µM), thus minimizing the possibility that the impairment of ATR by cholesterol was because of perturbation of binding of the ligand. In addition, the fact that A_2C normalizes cholesterol-enriched mitochondria membrane fluidity and restores the response to ATR indicate that cholesterol does not play a direct disturbing effect on ANT. Moreover, the reversing effect of A_2C provides additional evidence to discard changes in the physical parameters of the probes (*e.g.* lifetime of excited state) by cholesterol. Other examples for the regulation of membrane function by appropriate membrane fluidity have been reported (49, 50). Treatment of HEK cells with methyl-β-cyclodextrin, a cholesterol-extracting agent, fluidized the plasma membrane, as probed by DPH fluorescence anisotropy measurements, and enhanced the activity of α-secretase ADAM 10 (50).

Effect of Cholesterol on the Adenine Nucleotide Exchange Function of ANT—ANT constitutes the most abundant protein of the mitochondrial inner membrane and in physiological conditions ANT catalyzes the import of cytosolic ADP and the export of matrix ATP (51, 55). Therefore, we next examined the regulation by cholesterol of the adenine nucleotide transport. Freshly isolated rat liver mitochondria contain a physiological ATP concentration of 4–6 nmol/mg of protein, which did not change upon cholesterol loading, and hence we monitored the initial rate of ADP uptake into mitochondria. The uptake of ADP (in exchange for ATP) was linear for up to 1 min (not shown) and thus we examined the rate of ADP transport at

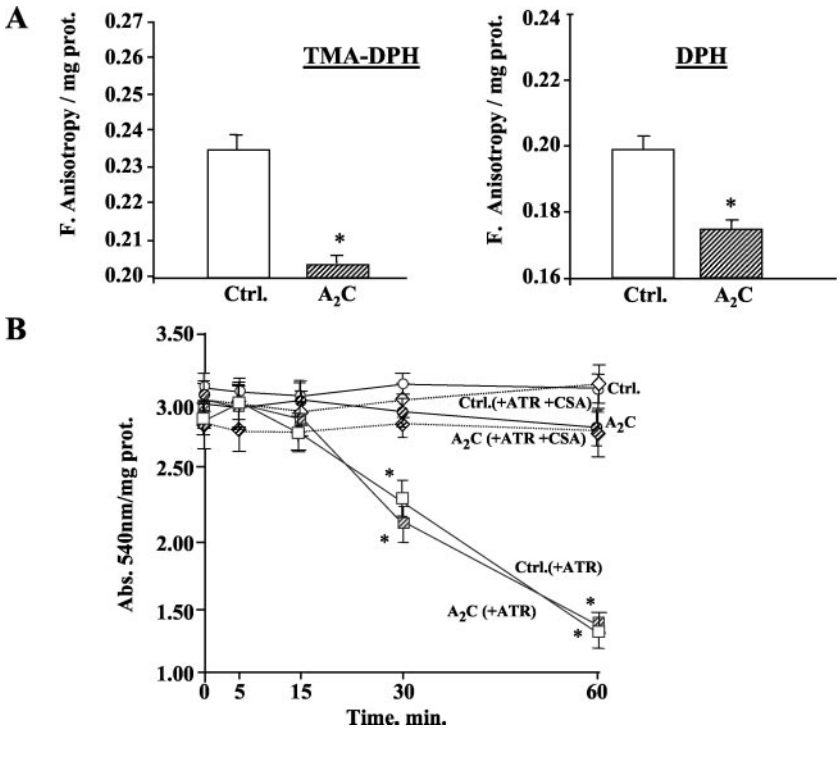

FIG. 7. **Fluidization of mitochondria does not modulate mitochondrial permeability transition.** Mitochondria (2 mg/ml) were incubated with A_2C (125 nmol/mg of protein) for 30 min at 37 °C. *A*, fluorescence anisotropy was determined using TMA-DPH and DPH as fluorescent probes. Results are presented as mean ± S.D. ($n = 6$). *, $p < 0.05$ *versus* control. *B*, parallel aliquots were incubated with ATR (100 μM) with or without pretreatment with CSA (5 μM, *dashed lines*) and mitochondrial swelling was determined by monitoring the absorbance at 540 nm over time. Results are presented as mean ± S.D. ($n = 6$). *, $p < 0.05$ *versus* control.

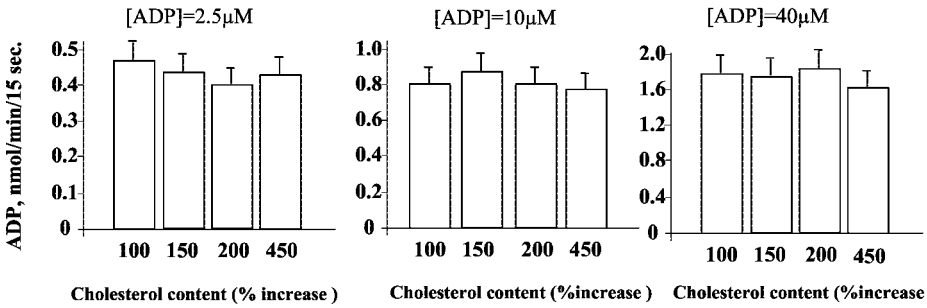

FIG. 8. **Adenine nucleotide transport rate in mitochondria loaded with cholesterol.** Mitochondria were loaded with increasing amounts of cholesterol as described in the legend to Fig. 3 and expressed as percentage increase over control (4.2 ± 0.8 μg of cholesterol/mg of protein, 100%) determining the initial rate of ADP uptake at the three concentrations shown as described under "Materials and Methods." Mitochondria were separated from medium by vacuum filtration and retained mitochondria were counted for radioactivity. Results are the mean ± S.D. of five to seven independent measurements.

three different concentrations of ADP (2.5–40 μM). The initial rate of ADP transport in control mitochondria increased with increasing concentrations of the substrate being similar to the reported V_{max} for ADP transport in rat liver mitochondria by ANT (56–59). Interestingly, the rate of ADP transport was not altered in mitochondria loaded with different amounts of cholesterol (Fig. 8) despite the fact that cholesterol dose dependently decreased membrane fluidity monitored by DPH fluorescence anisotropy (Fig. 3). Thus in contrast to the effect on mitochondrial swelling induced by ATR cholesterol loading does not perturb the ADT/ATP exchange function of ANT, thus establishing a divergent regulation of ANT by cholesterol-mediated changes in membrane fluidity.

The insensitivity of the adenine nucleotide exchange to conditions that alter mitochondrial membrane fluidity has been shown previously. Mitochondria from chronic alcohol-fed rat livers have decreased membrane fluidity because of altered mitochondrial lipid composition and cholesterol deposition (43, 60–62); the DPH fluorescence anisotropy values reported in these membranes were similar to the range we observed in our present observations. Consistent with the current findings the adenine nucleotide exchange in mitochondria from chronic alcohol-fed rats was unaltered (43, 63, 64), confirming that this transport function of mitochondria is not regulated by membrane fluidity.

An alternative possibility to the divergent regulation of ANT by cholesterol loading would imply that the impairment seen in the ATR-induced MPT could have been mediated by the effect of cholesterol on other putative MPT components that interact with ANT. There is considerable evidence supporting a role of ANT as a permeability transition pore component, although the precise molecular composition and regulation of permeability transition pore remain poorly understood (65). Current models indicate the interaction and association of ANT with outer mitochondrial membrane proteins including the VDAC and Bax (3–5, 66). In this regard, we observed that the release from mitochondria of cytochrome *c*, AIF, and Smac/Diablo induced by xanthine/xanthine oxidase-mediated superoxide anion generation, which has been shown to target VDAC (67), was independent of cholesterol loading and prevented by anti-VDAC antibody (25).[2] Thus, our data indicate a divergent sensitivity of ANT to membrane dynamics depending on its mode of action.

Concluding Remarks—The present study has relied on signature changes of MPT. Onset of MPT has a major consequence in

[2] A. Colell, C. García-Ruiz, and J. C. Fernández-Checa, unpublished observations.

the permeabilization of the inner mitochondrial membrane to small solutes. Thus, in addition to the dissipation of ion or metabolite gradient across the inner membrane, MPT results in a colloidal osmotic pressure that causes massive swelling, outer membrane rupture, and release of intermembrane proteins. The sensitivity to CSA stands as another important feature of regulated MPT (65). By monitoring these features we provide evidence that cholesterol deposition in mitochondria impairs the ATR-induced mitochondrial swelling and release of proapoptotic proteins that occur in control organelles. These dramatic changes induced by cholesterol are mediated by perturbation in mitochondrial membrane fluidity and not by cholesterol *per se* suggesting that an appropriate membrane fluidity range is needed for ATR to induce the conformational change in ANT that mediates MPT. An intriguing finding is that the ADP/ATP exchange function of ANT is insensitive to decreased mitochondrial membrane fluidity induced by cholesterol deposition. Accordingly these separated functions of ANT can be regulated independently and respond to cholesterol deposition in divergent ways. Consistent with these observations similar suggestions have been described for Bax-mediated regulation of ANT (68). The Bax-mediated inhibition of the ADP/ATP exchange was dissociated from Bax-stimulated formation of pores by ANT.

Being that MPT is an important gateway to cell death pathways, these observations may have important consequences in the control of cell death. According to the present findings mitochondrial cholesterol impairs the proapoptotic function of ANT without compromising the ADP/ATP exchange. Because stimulated ADP/ATP exchange has been shown to contribute to cell survival (69), our results imply that the divergent regulation of the two functions of ANT by cholesterol-mediated alteration in membrane fluidity may provide an advantage for cell survival. We would speculate that these conditions existing in certain tumor cells, *e.g.* Yoshida ascites and Morris hepatoma cells whose mitochondrial cholesterol levels are greater than in normal tissue (70, 71), may determine resistance to apoptosis stimuli that work through ANT.

Acknowledgments—We thank G. Kroemer and Y. Tsujimoto for kindly supplying anti-AIF and anti-VDAC (number 25) antibodies. The technical assistance of Anna Bosch and Marta Taulés, Serveis Cientifics Tecnics, and Susana Nuñez for help with immunoblots is greatly appreciated.

REFERENCES

1. Zoratti, M., and Szabò, I. (1995) *Biochim. Biophys. Acta* **1241,** 139–176
2. Bernardi, P. (1999) *Physiol. Rev.* **79,** 1127–1155
3. Beutner, G., Rück, A., Riede, B., and Brdiczka, D. (1998) *Biochim. Biophys. Acta* **1368,** 7–18
4. Marzo, I., Brenner, C., Zamzami, N., Jurgensmeier, J. M., Susin, S. A., Vieira, H. L. A., Prevost, M. C., Xie, Z., Matsuyama, S., Reed, J. C., and Kroemer, G. (1998) *Science* **281,** 2027–2031
5. O'Gorman, E., Beutner, G., Dolder, M., Koretsky, A. P., Brdiczka, D., and Walliman, T. (1997) *FEBS Lett.* **414,** 253–257
6. Kroemer, G., and Reed, J. C. (2000) *Nat. Med.* **6,** 513–519
7. Lemaster, J. J. (1999) *Am. J. Physiol.* **276,** G1–G6
8. Vieira, H. L., Haouzi, D., Hamel, C. E., Jacotot, E., Belzacq, A. S., Brenner, C., and Kroemer, G. (2000) *Cell Death Differ.* **7,** 1146–1154
9. Brenner, C., and Kroemer, G. (2000) *Science* **289,** 1150–1151
10. Green, D. R., and Reed, J. C. (1998) *Science* **281,** 1309–1312
11. Green, D. R. (1998) *Cell* **94,** 695–698
12. Liu, X., Kim, C. N., Yang, J., Jemmerson, R., and Wang, X. (1996) *Cell* **86,** 147–157
13. Li, P., Nijhawan, D., Budihardjo, I., Srinivasula, S. M., Ahmad, M., Alnemri, E. S., and Wang, X. (1997) *Cell* **91,** 479–489
14. Samali, A., Zhivotovsky, B., Jones, D. P., and Orrenius, S. (1998) *FEBS Lett.* **431,** 167–169
15. Susin, S. A., Lorenzo, H. K., Zamzami, N., Marzo, I., Brenner, C., Larochette, N., Prevost, M. C., Alzari, P. M., and Kroemer, G. (1999) *J. Exp. Med.* **189,** 381–394
16. Samali, A., Cai, J., Zhivotovsky, B., Jones, D. P., and Orrenius, S. (1999) *EMBO J.* **18,** 2040–2048
17. Susin, S. A., Lorenzo, H. K., Zamzami, N., Marzo, I., Snow, B. E., Brothers, G. M., Mangion, J., Jacotot, E., Constantini, P., Loeffler, M., Larochette, N., Goodlett, D. R., Aebersold, R., Siderovski, D. P., Penninger, J. M., and Kroemer, G. (1999) *Nature* **397,** 441–446
18. van Loo, G., Schotte, P., van Gurp, M., Demol, H., Hoorelbeke, B., Gevaert K., Rodriguez, I., Ruiz-Carrillo, A., Vandekerckhove, J., Declercq, W., Beyaert, R., and Vandenabeele, P. (2001) *Cell Death Differ.* **8,** 1136–1142
19. Du, C., Fang, M., Li, Y., Li, L., and Wang, X. (2000) *Cell* **102,** 33–42
20. Verhagen, A. M., Ekert, P. G., Pakush, M., Silke, J., Connoly, L. M., Reid, G. E., Moritz, R. L., Sympson, R. J., and Vaux, D. L (2000) *Cell* **102,** 43–53
21. van Loo, G., van Gurp, M., Depuydt, B., Srinivasula, S. M., Rodriguez, I., Alnemri, E. S., Gevaert, K., Vandekerckhove, J., Declercq, W., and Vandenabeele, P. (2002) *Cell Death Differ.* **9,** 20–26
22. Costantini, P., Bruey, J-M., Castedo, M., Métivier, D., Loeffler, M., Susin, S. A., Ravagnan, L., Zamzami, N., Garrido, C., and Kroemer, G. (2002) *Cell Death Differ***. 9,** 82–88
23. Waterhouse, N. J., Ricc, J. E., and Green, D. R. (2002) *Biochimie* (*Paris*) **84,** 113–121
24. Polster, B. M., Kinnally, K. W., and Fiskum, G. (2001) *J. Biol. Chem.* **276,** 37887–37894
25. Eskes, R., Antonsson, B., Osen-Sand, A., Montessuit, S., Richter, C., Sadoul, R., Mazzei, G., Nichols, A., and Martinou, J. C. (1998) *J. Cell Biol.* **143,** 217–224
26. Finucane, D. M., Waterhouse, N. J., Amarante-Mendes, G. P., Cotter, T. G., and Green, D. R. (1999) *Exp. Cell Res.* **251,** 166–174
27. Vander Heiden, M. G., Chandel, N. S., Williamson, E. K., Schumacker, P. T., and Thompson, C. B. (1997) *Cell* **91,** 632–643
28. Haworth, R. A., and Hunter, D. R. (1980) *J. Membr. Biol.* **54,** 231–236
29. Sugrue, M. M., and Tatton, W. G. (2001) *Biol. Signals Recept.* **10,** 176–188
30. Bernardi, P. (1992) *J. Biol. Chem.* **267,** 8834–8839
31. Huang, X., Zhai, D., and Huang, Y. (2001) *Mol. Cell. Biochem.* **224,** 1–7
32. Chernyak, B. V., Dedov, V. N., and Chernyak, V. Y.(1995) *FEBS Lett.* **365,** 75–78
33. Kristal, B. S., Park, B. K., and Yu, B. P. (1996) *J. Biol. Chem.* **271,** 6033–6038
34. Charnyak, B. V., and Bernardi, P. (1996) *Eur. J. Biochem.* **238,** 623–630
35. García-Ruiz, C., Colell, A., París, R., and Fernández-Checa, J. C. (2000) *FASEB J.* **14,** 847–858
36. García-Ruiz, C., Colell, A., Marí, M., Morales, A., and Fernández-Checa, J. C. (1997) *J. Biol. Chem.* **272,** 11369–11377
37. Pastorino, J. G., Marcineviciute, A., Cahill, A., and Hoek, J. B. (1999) *Biochem. Biophys. Res. Commun.* **265,** 405–409
38. Pastorino, J. G., and Hoek, J. B. (2000) *Hepatology* **31,** 1141–1152
39. Ricchelli, F., Gobbo, S., Moreno, G., and Salet, C. (1999) *Biochemistry* **38,** 9295–9300
40. Schnaitman, C. A., and Greenawalt, S. (1968) *J. Cell Biol.* **38,** 158–175
41. García-Ruiz, C., Morales, A., Ballesta, A., Rodés, J., Kaplowitz, N., and Fernández-Checa, J. C. (1994) *J. Clin. Invest.* **94,** 193–201
42. Aguilar, H. I., Botla, R., Arora, A. S., Bronk, S. F., and Gores, G. J. (1996) *Gastroenterology* **110,** 558–566
43. Colell, A., Garcia-Ruiz, C., Morales, A., Ballesta, A., Ookhtens, M., Rodes, J., Kaplowitz, N., and Fernandez-Checa, J. C. (1997) *Hepatology* **26,** 699–708
44. Martinez, F., Eschegoyen, S., Briones, R., and Cuellar, A. (1988) *J. Lipid Res.* **29,** 1005–1011
45. Duncan, I. W., Culbreth, P. H., and Burtis, C. A. (1979) *J. Chromatogr.* **162,** 281–292
46. Hildebrand, K., and Nicolau, C. (1979) *Biochim. Biophys. Acta* **553,** 365–377
47. Rouslin, W., MacGee, J., Gupte, S., Wesselman, A., and Epps, D. E. (1982) *Am. J. Physiol.* **242,** H254–H259
48. Blitterswijk, W. J., Wieb van der Meer, B., and Hilkmann, H. (1987) *Biochemistry* **26,** 1746–1756
49. Gimpl, G., Burger, K., and Farenholz, F. (1997) *Biochemistry* **36,** 10959–10974
50. Kojro, E., Gimpl, G., Lammich, S., Marz, W., and Farenholz, F. (2001) *Proc. Natl. Acad. Sci.* U. S. A. **98,** 5815–5820
51. Belzacq, A. S., Vieira, H. L. A., Kroemer, G., and Brenner, C. (2002) *Biochimie* (*Paris*) **84,** 167–176
52. Nicolli, A., Basso, E., Petronilli, V., Wenger, R. M., and Bernardi, P. (1996) *J. Biol. Chem.* **271,** 2185–2192
53. Van Blitterswijk, W. J., van Hoeven, R. P., and der Meer, B. W. (1981) *Biochim. Biophys. Acta* **644,** 323–332
54. Kosower, E. R., Kosower, N. S., and Wegman, P. (1977) *Biochim. Biophys. Acta* **471,** 311–319
55. Klingenberg, M. (1993) *J. Bioenerg. Biomembr.* **25,** 447–457
56. Lau, B. W. C., and Chan, S. H. P. (1984) *Cancer Res.* **44,** 4458–4464
57. Barbour, R. L., and Chan, S. H. P (1981) *J. Biol. Chem.* **256,** 1940–1948
58. Vignais, P. V., and Lauquin, G. J. M. (1979) *Trends Biochem. Sci.* **4,** 90–92
59. Klingenberg, M. (1976) in *The Enzymes of Biological Membrane: Membrane Transport* (Martonosi, A. N., ed) Vol. 3, pp. 383–438, Plenum, New York
60. Cunningham, C. C., Botenus, R. E., Spach, P. I., and Rudel, L. L. (1983) *Alcohol Clin. Exp. Res.* **7,** 424–430
61. Castro, J., Cortés, J. P., and Guzman, M. (1991) *Biochem. Pharmacol.* **41,** 1987–1995
62. Lluis, J. M., Colell, A., García-Ruiz, C., Kaplowitz, N., and Fernández-Checa, J. C. (2003) *Gastroenterology* **124,** 708–724
63. Cederbaum, A. I., and Rubin, E. (1975) *Fed. Proc.* **34,** 2045–2051
64. Gordon, E. (1977) *Biochem. Pharmacol.* **26,** 1229–1234
65. He, L., and Lemasters, J. J. (2002) *FEBS Lett.* **512,** 1–7
66. Crompton, M., Virji, S., and Ward, J. M. (1998) *Eur. J. Biochem.* **258,** 729–735
67. Madesh, M., and Hajnoczky, G. (2001) *J. Cell Biol.* **155,** 1003–1015
68. Belzacq, A. S., Vieira, H. L. A., Verrier, F., Vandecasteele, G., Cohen, I., Prevost, M. C., Larquet, E., Pariselli F., Petit, P. X., Kahn, A., Rizzuto, R., Brenner, C., and Kroemer, G. (2003) *Cancer Res.* **63,** 541–546
69. Vander Heiden, M. G., Chandel, N. S., Schumacker, P. T., and Thompson, C. B. (1999) *Mol Cell* **3,** 159–167
70. Feo, F., Canuto, R. A., Garcea, R., and Gabriel, L. (1975) *Biochim. Biophys. Acta* **413,** 116–134
71. Campbell, A. W., Capuano, A., and Chen, S. M. P. (2002) *Biochim. Biophys. Acta* **1567,** 123–132

Membrane Transport, Structure, Function, and Biogenesis:

Cholesterol Impairs the Adenine Nucleotide Translocator-mediated Mitochondrial Permeability Transition through Altered Membrane Fluidity

Anna Colell, Carmen García-Ruiz, Josep M. Lluis, Olga Coll, Montse Mari and José C. Fernández-Checa

J. Biol. Chem. 2003, 278:33928-33935.
doi: 10.1074/jbc.M210943200 originally published online June 23, 2003